J Mater Sci (2010) 45:6812–6818
DOI 10.1007/s10853-010-4779-7

Cu(II), Co(II) and Ni(II) complexes of –Br and $–OCH_2CH_3$ substituted Schiff bases as corrosion inhibitors for aluminium in acidic media

A. Aytaç

Received: 22 February 2010 / Accepted: 19 July 2010 / Published online: 30 July 2010

Abstract A group of Cu(II), Ni(II) and Co(II) complexes of –Br and $–OCH_2CH_3$ substituted Schiff bases as a new class of corrosion inhibitors for aluminium has been studied in 0.1 M HCl by the addition of 10 ppm compound using potentiodynamic polarization, electrochemical impedance spectroscopy, linear polarization methods and gas evolution tests at 25 °C. The inhibition efficiencies obtained from all methods employed are in good agreement. Results show Ni(II) complex of $–OCH_2CH_3$ substituted Schiff bases was the best inhibitor with a mean efficiency of 69% at 10 ppm additive concentration. The potentiodynamic polarization curves showed both the cathodic and the anodic processes of aluminium corrosion were suppressed, and the Nyquist plots of impedance gave mainly a capacitive loop. Scanning electron microscopy (SEM) was done from the surface of the exposed sample indicating uniform film on the surface.

Introduction

The most important feature of aluminium is its corrosion resistance due to the presence of a thin, adherent and protective surface oxide film. Owing to this advantage, aluminium and its alloys have a wide range of industrial applications such as reaction vessels, pipes, machinery and chemical batteries. The pickling, chemical and the electrochemical etching of aluminium are carried out with hydrochloric acid solutions. The solubility of the protective oxide film upon the Al surface increases above and below pH 4–9 [1–3] range and aluminium exhibits a uniform attack. Inhibitors are used to prevent metal dissolution and minimize acid consumption.

Some Schiff bases have recently reported as effective corrosion inhibitors for steel [4–9], aluminium [10], aluminium alloys [11, 12] and copper [13] in acidic media. Due to the presence of the –C=N– group, electronegative nitrogen, sulphur and/or oxygen atoms in the molecule, Schiff bases are good corrosion inhibitors. The action of such inhibitors depends on the specific interaction between the functional groups and the metal surface. So it is very important to clarify the interactions between inhibitor molecules and metal surfaces in order to search new and efficient corrosion inhibitors. Theoretical approaches provide means of analysing these interactions, and there are many reports related with this area [14–21]. The main results showed that some mechanical properties depend on the electronic and structural properties of the inhibitor molecule such as aromatic and functional groups, electron density on donor atoms and л orbital character of donating electrons [12, 13].

In this article, metal-free –Br and $–OCH_2CH_3$-substituted Schiff bases and their Cu(II), Ni(II) and Co(II) complexes were selected as corrosion inhibitor of aluminium. The correlations between the chemical structures of complex compounds, their inhibiting efficiency in respect to acidic corrosion of aluminium are discussed on the basis of the electrochemical impedance spectroscopy (EIS), potentiodynamic polarization, linear polarization data and gas evolution tests. Surface morphology was investigated by scanning electron microscopy (SEM) method.

A. Aytaç (✉)
Department of Chemistry, Faculty of Science, Gazi University, Teknikokullar, Ankara 06500, Turkey
e-mail: aylin.aytac@gmail.com

A. Aytaç
Department of Materials Technology and Electrochemistry, Norwegian University of Science and Technology, Sem Saelands vei 6, 7491 Trondheim, Norway

Experimental details

Preparation of the Schiff bases and complexes

High purity grade commercial 2-aminophenol and aldehydes as well as Cu(II), Ni(II) and Co(II) chlorides from Aldrich Chemical Co. were used without further purification.

The metal-free –Br and $–OCH_2CH_3$ substituted Schiff bases APh-Br and APh-OCH_2CH_3 were obtained by the following procedure: The solution mixture of 2-aminophenol (1 mmol) and the aldehyde (1 mmol) was refluxed with stirring for 1 h in 50 mL of dioxan. After removing the 10 mL solvent, the solid was filtered and washed with diethyl ether, and then the solid was dried in vacuum at room temperature. The yield was 78%.

The metal complexes of Schiff bases were obtained as follows. A solution of $MCl_2{\cdot}nH_2O$ (1.25 mmol, M: Cu(II), Ni(II) and Co(II)) in 25 mL methanol and the solution of Schiff bases (1.25 mmol) in 25 mL methanol were mixed. These mixtures were stirred for 1 h. After 2 h later, the solids were filtered and washed with ethanol then with dioxan and the solids were dried at room temperature in desiccator. Yields 54%. The molecular structure of Schiff bases and metal complexes are shown in Fig. 1a and b.

According to our earlier studies Co(II) complex shows a tetrahedral structure and the complexes of Ni(II) are diamagnetic suggesting a square-planer geometry [22]. There are two different structures for five coordinate Cu(II) complexes these are the square pyramid and the trigonal bipyramid [20].

Electrochemical measurements

The sample selected for the study was 99.998% pure aluminium. The 2 × 0.5 × 0.3 cm dimension of specimens was used for electrochemical techniques. Prior to each experiment, the surface pre-treatment of Al specimens was performed by mechanical polishing (using a polishing machine) of the electrode surface with successive grades of emery papers down to 1200 grit up to a mirror finish. The electrodes were then rinsed with acetone and distilled water and dried at room temperature.

Electrochemical impedance (EIS) measurements, potentiodynamic polarization, linear polarization studies were carried out using Volta Lab PGZ 301 electrochemical analyzer. Electrochemical experiments were performed in a conventional three electrodes electrochemical cell. The counter and reference electrodes were platinum plate (2 cm^2) and Ag/AgCl electrode, respectively. The impedance measurements were carried out 5 mV (rsm) applied voltage of sinusoidal wave in frequency range 20 kHz–50 mHz at 25 °C. The EIS measurements were conducted after 30 min immersion in experimental solution that ensured a system in equilibrium. Potentiodynamic polarization studies were performed with a scan rate of 5 mV/s in the potential range from −1200 to −600 mV relative to the corrosion potential. Experiments were always repeated at least three times. All compounds studied were put in the 0.1 M HCl at concentration of 10 ppm. The Schiff bases used in this study were specially synthesized and investigated their small concentration on aluminium corrosion. They have high molecular weights the amount to be added in the corrosion test cell was determined as 10 ppm.

In order to determine the polarization resistance, R_p, the potential of the working electrode was ramped ±20 mV near E_{corr} at a scan rate of 0.5 mV/s. Rp obtained from polarization techniques was determined simultaneously by Volta Lab PGZ 301 electrochemical analyzer software.

Gas evolution tests

The inhibiting effect of some Schiff bases and the complexes on the corrosion of aluminium in 0.1 M HCl has

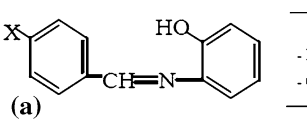

X	*Name*	*Abbreviation*
- Br	N-4-bromobenzilidene-2-aminophenol	APh-Br
- OCH_2CH_3	N-4-ethoxybenzilidene-2-aminophenol	APh-OCH_2CH_3

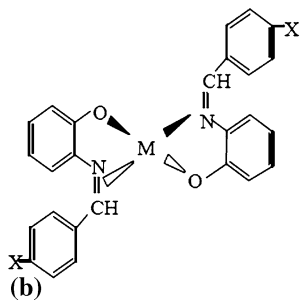

Metal (M)	*Co*	*Ni*	*Cu*
Abbreviation	[Co(APh-OCH_2CH_3)] [Co(APh-Br)]	[Ni(APh-OCH_2CH_3)] [Ni(APh-Br)]	[Cu(APh-OCH_2CH_3)] [Cu(APh-Br)]

Fig. 1 Structure of the Schiff bases (**a**); the M(II) complexes derived from Schiff bases (**b**)

been studied by means of the hydrogen evolution measurement. The 2 × 0.5 cm dimension of specimens was used for gas evolution test. Prior to each experiment, the surface pre-treatment of Al specimens was performed by mechanical polishing of the electrode surface with successive grades of emery papers down to 1200 grit up to a mirror finish. The electrodes was then rinsed with acetone, distilled water and dried at room temperature.

For hydrogen evolution test, a U-shaped test apparatus was set up. The sample was immersed into a tube containing 30 mL, 0.1 M HCl solution and was connected to the apparatus. During hydrogen evolution at 25 °C, the changes in the volume of the system were measured as mm of H_2O at constant air pressure.

SEM and EDS analysis

The specimens used for surface morphology examination were immersed in 0.1 M HCl, containing 10 ppm Schiff base and blank, for 48 h. Then, they have been removed, rinsed quickly with 98% ethanol and dried under 300 K. The analysis was performed on a Hitachi SI-3500 N SEM with an INCA energy X-ray spectrometer. The accelerating voltage was 20 kV.

Results and discussions

Electrochemical impedance spectroscopy

The corrosion behaviour of aluminium in 0.1 M HCl solution in the presence of 10 ppm Schiff bases and the complexes was investigated using EIS at open circuit potential. Nyquist plots are given in Fig. 2. It is clear from the plots that the impedance response changes with the addition of the compounds. The polarization resistance (R_p) and inhibition efficiency ($\eta\%$) values of the Schiff bases and the complexes in 0.1 M HCl solution were calculated from Eq. 1 and given in Table 1.

$$\eta_{imp}(\%) = \frac{R_p - R_p^o}{R_p} \times 100 \quad (1)$$

where R_p and R_p^o denote polarization resistance of electrode with and without inhibitor, respectively, evaluated from Nyquist diagrams using circular recreation analysis.

As we notice from Fig. 2 all the plots display a single capacitive loop, the impedance diagrams show semi-circles indicating a barrier layer formed on the surface and a charge transfer process mainly controlling the corrosion of aluminium. (APh-Br) and Ni(APh-Br) comprise one completed inductive loop at low frequencies. All other impedance spectra had only capacitive loop and had a tendency to give an inductive loop [10, 23]. High frequency capacitive loop was attributed to the charge transfer of the corrosion process and to the formation of an oxide layer whilst low frequency inductive loop was often attributed to the surface relaxation of species in the oxide layer [24] or related to stabilizations of layer by adsorbed intermediate products of the corrosion reaction on the electrode surface involving inhibitor molecules as well as reactive products [25]. The diameter of the semi-circles decreases in the order [Ni(APh-OCH_2CH_3)] > [Cu(APh-OCH_2CH_3)] > [Cu(APh-Br)] > [Ni(APh-Br)] > (APh-Br) > [Co(APh-Br)]) > [Co(APh-OCH_2CH_3)] > (APh-OCH_2CH_3) depending on the influence of the structure at the certain concentration. This response can be possibly explained by the organization of the molecules adsorbed to the electrode surface.

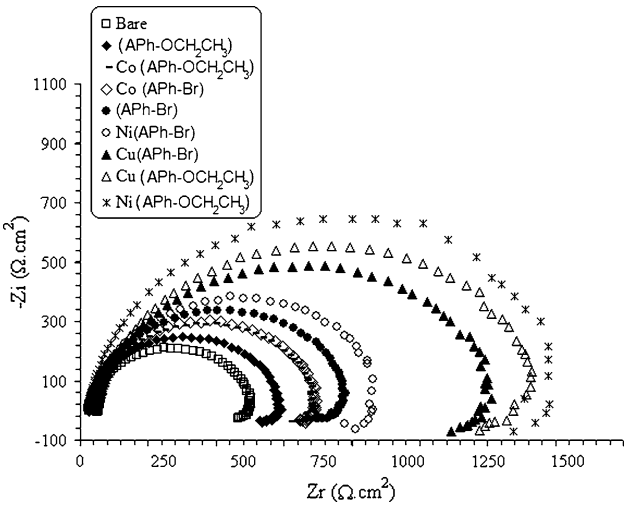

Fig. 2 Nyquist diagrams for aluminium in 0.1 M HCl containing without and with Schiff bases and their Cu, Co and Ni metal complexes at 25 °C

Table 1 Impedance parameters and corresponding inhibition efficiency for the corrosion of aluminium in 0.1 M HCl at 25 °C

Inhibitor	R_p (ohm cm^2)	$\eta(R_p)\%$
Bare	491	–
[Ni(APh-OCH_2CH_3)]	1487	67
[Cu(APh-OCH_2CH_3)]	1444	66
[Cu(APh-Br)]	1292	62
[Ni(APh-Br)]	926	47
(APh-Br)	832	41
[Co(APh-OCH_2CH_3)]	712	31
[Co(APh-Br)]	701	30
(APh-OCH_2CH_3)	585	16

Equivalent circuit analysis

Experimental plots have a depressed semicircular shape in the complex impedance plane, with the centre under the real axis. This behaviour is typical for solid metal electrodes that show frequency dispersion. Electrical equivalent circuits are generally used to model the electrochemical behaviour and to calculate the parameters of interest. There are two ways to describe the EIS spectra for the inhomogeneous films on the metal surface or rough and porous electrodes. One is the finite transmission line model and the other is the filmed equivalent circuit model, which is usually proposed to study the degradation of coated metals [26]. It has been suggested that the impedance spectra for the metal covered by organic inhibitor films are very similar to the failed coating metals [23, 27]. Therefore, in this study the filmed equivalent circuit model is used to describe the inhibitor-covered metal/solution interface.

The equivalent circuit model used to fit the experimental results is shown in Fig. 3. It consists of solution resistance, R_s, a constant phase element, Q, in parallel with polarization resistance R_p and R_{ind}, and an inductance, L, in parallel with R_{ind}, and L can be correlated with low frequency intermediate process.

When discussing inhibition action of inorganic compounds various factors must be taken into consideration [10, 28]. These include the number of functional groups taking part in the adsorption of the inhibitor molecule and their electron charge density, molecular size and geometry and mode of interaction.

The order of inhibition efficiency for the tested compounds as revealed from Figs. 4, 5 and 6 is: [Ni(APh-OCH_2CH_3)] > [Cu(APh-OCH_2CH_3)] > [Cu(APh-Br)] > [Ni(APh-Br)] > (APh-Br) > [Co(APh-Br)]) > [Co(APh-OCH_2CH_3)] > (APh-OCH_2CH_3).

From the data of Table 1, 2 and 3, the observed inhibition efficiency indicate that most of the complexes have higher inhibition activity than the free ligand. Such an increased activity of the metal chelates can be explained on the basis of the chelation theory. On chelation, the polarity of the metal ion will be reduced to a greater extent due to the overlap of the ligand orbital and partial sharing of the positive charge of the metal ion with donor groups. Further, this increases the delocalization of p electrons over the whole chelate ring.

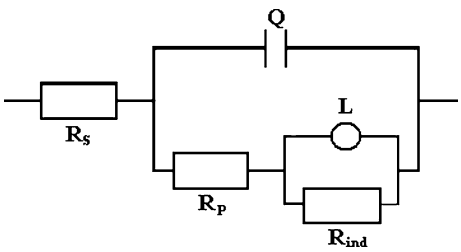

Fig. 3 Electrochemical equivalent circuit diagram for metal–electrolyte interface

Moreover, it is evident that molecular geometry plays an important role in the inhibition process. To explain this order it may be stated that the presence of the metals affects the inhibition action greatly. [Ni(APh-OCH_2CH_3)] molecules adsorb more strongly than the others because it is probably favour the flat orientation over the metal surface so in this orientation it has the largest number of free adsorbing oxygen, nitrogen atoms and π electrons through which the adsorption process may be achieved due to their high electronegativity.

The electronic spectra of the Co(II) complex shows an absorption band at around 400 nm, which is compatible with this complex having a tetrahedral structure [20]. The complexes of Ni(II) are diamagnetic suggesting square-planer geometry. The electronic spectra of the Ni(II) complexes shows an absorption band at *ca.* 520 nm, corresponding for square-planar geometry nickel compounds [21]. Cu(II) complexes are five coordinated these with ligands. The electronic spectra of the Cu(II) complex shows absorption band at 715 nm corresponding for the square-based pyramidal Cu(II) configuration [28, 29]. The low values of the room temperature magnetic moments of Cu(II) complexes may be due to an intermolecular interaction complexes of Cu(II) with ligands [29].

The difference in inhibition efficiency lies mostly in the geometry and the size of the organic compound—Ni(II) complex having square-planar geometry and being larger planar surface and hence more effective. Efficient adsorption is the result of p electrons of the aromatic system, double bonds and electronegative nitrogen and oxygen atoms present in the structure. During chemisorption of the compounds, electron transfer can be expected with compounds having relatively loose band electrons. The p electrons in the system are then likely to be the determining factor in the inhibition efficiency.

Polarization measurement

Potentiodynamic polarizations were carried out on the inhibition of aluminium in 0.1 M HCl solution with 2-aminophenol-Schiff basses and their metal complexes. In order to better define the action of different additives on the corrosion process a series of anodic and cathodic polarization curves were recorded after an immersion of 30 min. It can be seen from Fig. 4 that both anodic and cathodic current densities were obtained in 0.1 M HCl solutions in the presence of Schiff bases.

The electrochemical parameters such as corrosion potential (E_{corr}), corrosion current density (i_{corr}) cathodic

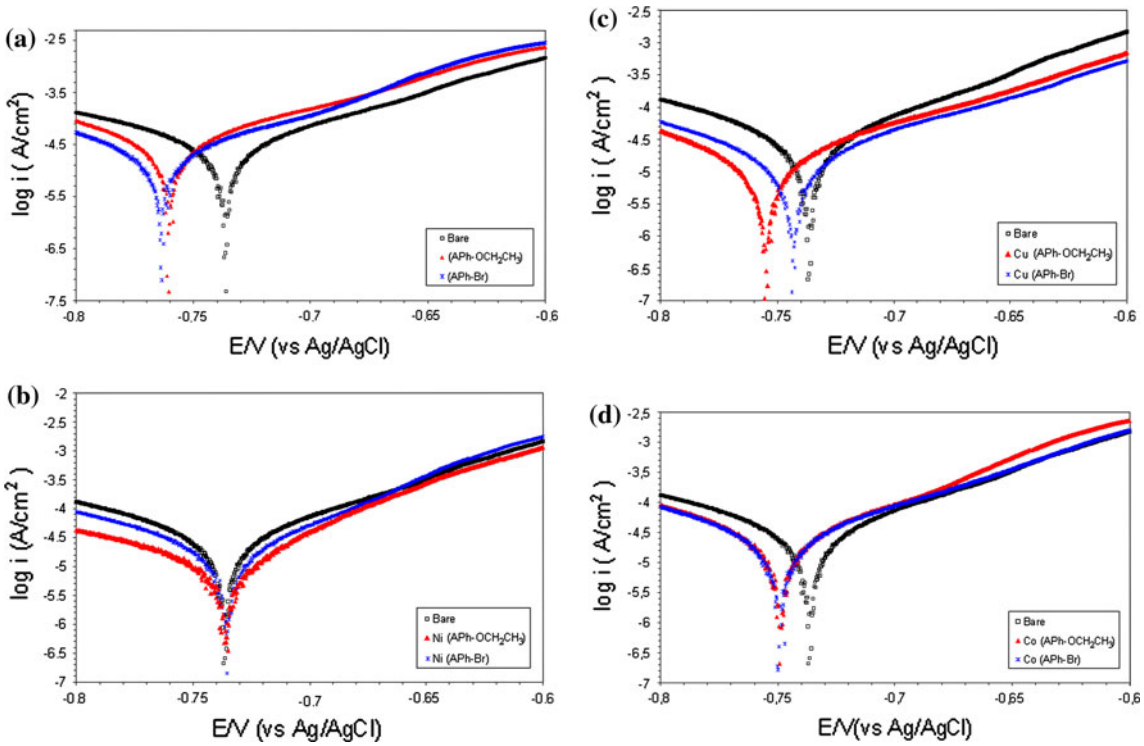

Fig. 4 Polarization curves for aluminium in 0.1 M in the presence of **a** substituted –Br and $–OCH_2CH_3$ schiff bases and **b** Ni, **c** Cu and **d** Co metal complexes (10 ppm) at 25 °C

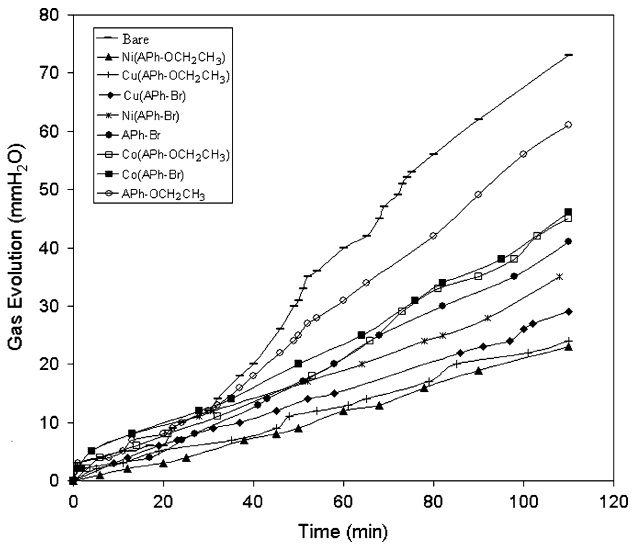

Fig. 5 The time depends of volume of hydrogen evolution of aluminium with addition of inhibitors at 10 ppm concentration in 0.1 M HCl

(β_c) and anodic Tafel slope (β_a) obtained from polarization curves, and corresponding inhibition efficiency ($\eta\%$) values are given in Table 2. The inhibition efficiency at different inhibitors was calculated from equation:

$$\eta_{pol}\% = \frac{i_{corr} - i_{corr(inh)}}{i_{corr}} \quad (2)$$

where i_{corr} and $i_{corr(inh)}$ are the corrosion currents without and with inhibitor, respectively. The inhibition efficiency value of the examined Schiff bases follows the order [Ni(APh-OCH_2CH_3)] > [Cu(APh-OCH_2CH_3)] > [Cu(APh-Br)] > [Ni(APh-Br)] > (APh-Br) > [Co(APh-Br)]) > [Co(APh-OCH_2CH_3)] > (APh-OCH_2CH_3) as impedance measurement results.

It is also observed from Table 2 that E_{corr} values and Tafel slope constants β_a and β_a do not change significantly in inhibited solution as compared to uninhibited solution.

The inhibition efficiency depends on many factors including adsorption centres, mode of interaction, molecular size and structure [6, 10]. The effect of molecular size and structure can easily be viewed from the difference in the structure of compound Ni complex with respect to other compounds.

Linear polarization measurement

In order to determine the polarization resistance, R_p, the potential of the working electrode was ramped ± 20 mV near E_{corr} at a scan rate of 0.5 mV/s. Polarization resistance, R_p, values for aluminium in HCl solution in the presence and in the absence of inhibitor were also determined using linear polarization method. The results shown in Table 2 indicate that the addition of all the examined Schiff bases causes an increase in polarization resistance.

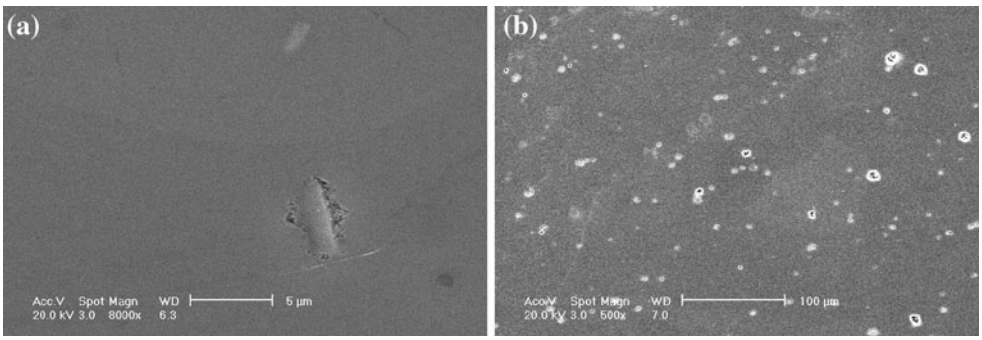

Fig. 6 The surface (SEM micrographs) of the aluminium **a** 0.5 M HCl, **b** 0.5 M HCl + 10 ppm [Ni(APh–OCH_2CH_3)] at 25 °C, immersion time was 48 h

Table 2 Polarization parameters and the corresponding inhibitor efficiencies for aluminium in 0.1 M HCl containing of the Schiff bases

Inhibitor	Potentiodynamic polarization						Linear polarization	
	i_{corr} (μA/cm^2)	E_{corr} (mV)	$-\beta_c$ (mV/dec)	β_a (mV/dec)	C.R. (mm/y)	η%	R_p (ohm cm^2)	η_{Rp} %
Bare	28.16	−737.2	−80.9	77.9	306.1	–	596	
[Ni(APh-OCH_2CH_3)]	8.64	−736.9	−80.1	53.6	93.94	69.3	1280	53.4
[Cu(APh-OCH_2CH_3)]	9.60	−755.7	−68.9	64.4	104.4	65.9	1200	50.3
[Cu(APh-Br)]	11.69	−744.1	−78.3	74.9	127.1	58.5	1080	44.8
[Ni(APh-Br)]	14.05	−736.3	−74.4	63.2	152.8	50.1	901	33.8
(APh-Br)	18.9	−764.7	−55.3	79.3	205.5	32.9	752	20.7
[Co(APh-Br)]	19.12	−750.1	−79.3	74.5	207.9	32.1	671	11.2
[Co(APh-OCH_2CH_3)]	21.03	−749.7	−80.9	74.3	228.7	25.3	622	4.3
(APh-OCH_2CH_3)	23.82	−761.1	−64.5	73.9	259.0	15.4	618	3.6

Table 3 Inhibitor efficiencies for 10 ppm of corresponding inhibitors for the corrosion of aluminium in 0.1 M HCl from gas evolution tests

Inhibitor	H_2 evolution rate mm/min	$\eta(R_p)$%
Bare	0.652	–
[Ni(APh-OCH_2CH_3)]	0.196	70
[Cu(APh-OCH_2CH_3)]	0.209	68
[Cu(APh-Br)]	0.261	60
[Ni(APh-Br)]	0.313	52
(APh-Br)	0.359	45
[Co(APh-OCH_2CH_3)]	0.391	40
[Co(APh-Br)]	0.404	38
(APh-OCH_2CH_3)	0.522	20

The polarization resistance values were determined from the slope of the current density–potential plots from the slope of current density potential plots. Table 3 shows that the polarization resistance decreases the order [Ni(APh-OCH_2CH_3)] > [Cu(APh-OCH_2CH_3)] > [Cu(APh-Br)] > [Ni(APh-Br)] > (APh-Br) > [Co(APh-Br)]) > [Co(APh-OCH_2CH_3)] > (APh-OCH_2CH_3), in the presence of all compounds, indicating adsorption of the inhibitor on the metal surface to block the active sites and inhibit corrosion. Results show that Ni(APh-CH_2CH_3) is the most efficient inhibitor at 10 ppm concentration. Inhibition efficiency values calculated from potentiodynamic polarization and linear polarization methods have the same order.

Gas evolution tests

Figure 5 shows the volume of hydrogen evolution of aluminium after 2 h with addition of Schiff bases and the complexes at 10 ppm concentration. All aluminium specimens were put into 50 mL 0.1 M HCl solution at room temperature. The slopes of these curves can be taken as the rate of aluminium corrosion (Table 3). All these curves show steady-state hydrogen evolution rate after a certain period of time.

The inhibition efficiencies were calculated from the data using equation,

$$\eta_{H_2}(\%) = \frac{R_0 - R}{R_0} \times 100 \quad (3)$$

where R is the corrosion rate in the presence of inhibitor and R_o the corrosion rate without inhibitor. R and R_o values

were determined from the slopes of the hydrogen evolution curves for all inhibitors. The R_o was 0.652 mm min^{-1}.

It is obvious from Fig. 4 that Ni(APh-CH_2CH_3) is the most efficient inhibitor, and it reduced the hydrogen evolution when compared with others. It is also clear that the corrosion rates decrease with the addition of these inhibitors when compared with standard solution.

SEM analysis

Scanning electron microscopy studies of the alloy surface in the absence (Fig. 6a) and presence of [Ni(APh-OCH_2CH_3)], which has highest inhibition efficiencies (Fig. 6b), were performed to examine the nature of the film on the surface. The SEM reveals the presence of some pits on the surface of the aluminium in the absence of inhibitor whilst such pits are not seen in the presence of inhibitor. This indicated that there is an adsorption layer formed and it protects the specimen surface after immersion in the acid containing [Ni(APh-OCH_2CH_3)]; so the oxidation and corrosion of aluminium is lightly in comparison with that in blank.

Conclusions

The principle conclusions can be summarized as follows.

1. A group of Cu(II), Ni(II) and Co(II) complexes of –Br and –OCH_2CH_3 substituted Schiff bases as a new class of corrosion inhibitors for aluminium has been studied in 0.1 M HCl by the addition of 10 ppm compound using potentiodynamic polarization, electrochemical impedance spectroscopy, linear polarization methods and gas evolution tests. All the schiff bases studied are found to perform as a corrosion inhibitor in hydrochloric acid solution, and the inhibiting efficiency values of the examined Schiff bases follow the order [Ni(APh-OCH_2CH_3)] > [Cu(APh-OCH_2CH_3)] > [Cu(APh-Br)] > [Ni(APh-Br)] > (APh-Br) > [Co(APh-Br)]) > [Co(APh-OCH_2CH_3)] > (APh-OCH_2CH_3) at the concentration of 10 ppm. [Ni(APh-OCH_2CH_3)] was found to be effective inhibitors for aluminium corrosion in 0.1 M HCl.
2. The three different techniques showed a good agreement with each other and yield nearly the same values of $\%\eta$. Maximum efficiency is 69% for Ni complex for 10 ppm.
3. Scanning electron photographs in the presence of [Ni(APh-OCH_2CH_3)] showed a good surface coverage on the metal surface.

Acknowledgements The author thanks NTNU inorganic department for their help. This project was supported by TÜBITAK (project no.MAG107M476).

References

1. Pourbaix M (1966) Atlas of electrochemical equilibria in aqueous solutions. Pergamon Press, New York
2. Obot IB, Obi-Egbedi NO, Umoren SA (2009) Corros Sci 51:1868
3. Obot IB, Obi-Egbedi NO (2008) Colloids Surf A Physicochem Eng Asp 330:207 (2008)
4. Behpour M, Ghoreishi SM, Gandomi-Niasar A et al (2009) J Mater Sci 44:2444. doi:10.1007/s10853-009-3309-y
5. Fu JJ, Li SN, Cao LH et al (2010) J Mater Sci 45:979. doi:10.1007/s10853-009-4028-0
6. Umoren S, Obot I, Obi-Egbedi N (2009) J Mater Sci 44:274. doi:10.1007/s10853-008-3045-8
7. Amin MA, Abd El Rehim SS, El-Naggar MM, Abdel-Fatah HTM (2009) J Mater Sci 44:6258. doi:10.1007/s10853-009-3856-2
8. Wang CY, Wu GH, Zhang Q et al (2008) J Mater Sci 43:3327. doi:10.1007/s10853-008-2506-4
9. Hahner G, Woll Ch, Buck M, Grunze M (1993) Langmuir 9(1):955
10. Aytac A, Ozmen U, Kabasakaloglu M (2005) Mater Chem Phys 89:176
11. Li SL, Chen S, Lei SB, Ma H, Yu R, Liu D (1999) Corros Sci 41:1273
12. Wang D, Li S, Ying Y, Wang M, Xiao H, Chen Z (1999) Corros Sci 41:1911
13. Bentis F, Lagreene M, Elmehdi B, Mernari B, Traisnel M, Vezin H (2002) Corrosion 58:399
14. Thunhorst M, Holzgrabe U (1998) Magn Reson Chem 36:153
15. Bolvig S, Hansen PE (1996) Magn Reson Chem 34:419
16. Silverstein RM, Bassler GC, Morrill TC (1981) Spectrophotometric identification of organic compounds, 4th edn. Wiley, New York
17. Lal RA, Adhikari S, Chakraborty J (2001) Synth React Inorg Met-Org Chem 31:65
18. Nakamoto K (1986) Infrared and Raman spectra of inorganic and coordination compounds, 4th edn. Wiley, New York
19. Issa RM, Abdel-Latif SA, Abdel-Salam HA (2001) Synth React Inorg Met-Org Chem 31:95
20. Cotton FA, Wilkinson G (1972) Advanced inorganic chemistry, 3rd edn. Wiley, London
21. Lever ABP (1984) Inorganic electronic spectroscopy. Elsevier, New York, NY
22. Sari N, Aytaç A (2009) Asian J Chem 21:839
23. Lee EJ, Pyun SI (1995) Corros Sci 37:157
24. Abd El-Rehim SS, Hassan HH, Amin MA (2001) Mater Chem Phys 70:64
25. Langmuir I (1917) J Am Chem Soc 39:1848
26. Metikos-Hukovic M, Babic R, Grubac Z (2002) J Appl Electrochem 32:35
27. Gojic M, Horvat R, Metikos-Hukovic M (1995) Proceedings of the Eighth European Symposium on Corrosion Inhibitors (8 SEIC), Ann. Univ. Ferrrara, N.S. V, Suppl. N. 10, 1995, p 97
28. El-Sayed AB, Abo-Aly MM, Attia GM (2001) Synth React Inorg Met-Org Chem 31:1565
29. Yamada S, Kuge Y, Yamanouchi K (1967) Inorg Chem Acta 1:139